The 17th International Workshop on Water Waves and Floating Bodies, Cambridge, UK, April 2002

First- and Second-Order Water Waves Around an Array of Floating Vertical Cylinders

Masashi Kashiwagi and Yuhki Ohwatari

Research Institute for Applied Mechanics, Kyushu University
Fukuoka 816-8580, Japan E-mail: *kashi@riam.kyushu-u.ac.jp*

ABSTRACT

Spatially dense measurements are carried out for the free-surface elevation around four truncated circular cylinders equally spaced along a straight line. At each of three wavelengths selected after preliminary measurements, two different waves in amplitude are generated with wave steepness H/λ set approximately to 1/50 and 1/20. Through comparison with computed results, discussion is made on the characteristics in the spatial distribution of the first- and second-order waves and validity of the potential-flow computations around near-trapping frequencies.

1. INTRODUCTION

Understanding hydrodynamic interactions among multiple floating bodies is important in a study of column-supported type very large floating structures. Recent numerical computations predict very large free-surface elevation and wave forces due to hydrodynamic resonant phenomena at some critical frequencies.

To confirm whether this is true, some experimental measurements have been carried out using arrays of a number of elementary bodies placed at regular intervals. For example, Kashiwagi & Yoshida [1] measured spatial variation of the wave elevation along the longitudinal centerline of a structure which consists of 64 vertical circular cylinders arranged in an array of 4 rows and 16 columns. On the whole, good agreement was found between computed and measured results. However, the measured wave amplitudes were much smaller than the computed ones around a critical frequency where the wave resonant phenomenon was observed in an interior region of the array (which is known at present as the near-trapping frequency). This discrepancy was attributed vaguely to viscous effects or nonlinear effects. To make clear these ambiguous points, more thorough investigation is needed both in numerical computations and experiments.

In the present paper, using a model composed of four truncated circular cylinders which are equally spaced along a straight line, the wave elevation around each cylinder is measured densely in space by traversing gradually the positions of wave probes. Measured time histories are Fourier analyzed, separating into quantities with the first-harmonic (first-order) and second-harmonic (second-order) of the wave frequency. Numerical computations corresponding to the experiments are also performed. With these results, discussion is made on the degree of agreement in the first- and second-order wave elevations and on their characteristics.

2. EXPERIMENTS

A model used in experiments consists of four vertical circular cylinders with horizontal base, as schematically shown in Fig. 1. The radius, diameter, and draft of an elementary circular cylinder are denoted as a, $D\,(=2a)$, and d, respectively, and the separation distance between the axes of adjacent cylinders is denoted as $2s$. Then the tested model was set as $D = 165$ mm, $d = 2D$, and $s = D$. The whole model was rigidly fixed to a measuring carriage, with the longitudinal line of the array (x-axis) set equal to the longitudinal centerline of a wave tank.

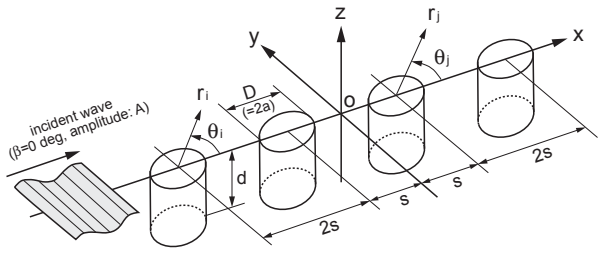

Fig. 1 Coordinate system and notations

The incident waves in experiments are all plane progressive waves (the amplitude and the angle of attack are denoted as A and β respectively), and measurements were conducted in head waves, i.e. $\beta = 0^\circ$. To see nonlinear effects, two different amplitudes were set for each wavelength such that the wave steepness (the ratio of wave height $H = 2A$ to wave length λ) was approximately equal to 1/50 and 1/20.

For spatially dense measurement of the wave elevation, three units of the wave measuring apparatus were prepared, each of which consists of five wave probes of capacitance type placed at regular intervals of 35 mm. By traversing these measuring apparatus in the y-axis with interval of 20 mm (only the outermost tip is separated by 25 mm), the wave elevation was measured at 305 positions in total, the positions of which are shown in Fig. 2. In reality, the measurements were carried out twice; the number of measured positions in the first experiment is 225, which are shown by closed circles (•) in Fig. 2. Since we realized after data analyses that these 225 points were not enough for spatial resolution of the wave pattern, additional 80 positions shown by open circles (○) in Fig. 2 were chosen for the second measurement. In addition to these measurements around circular cylinders, the amplitude of incident

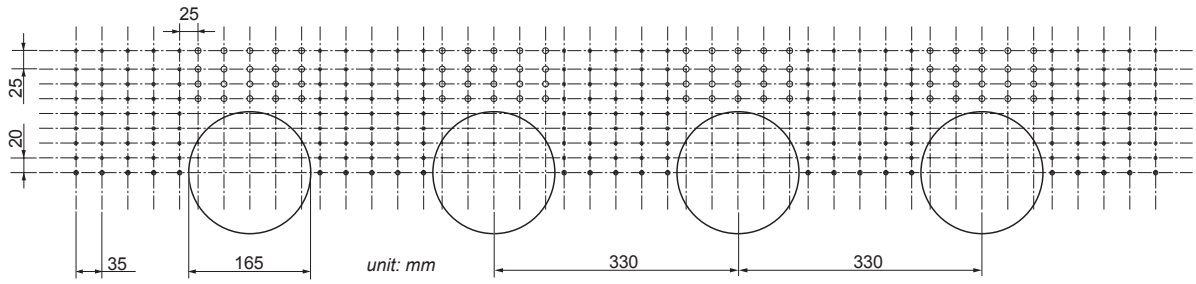

Fig. 2 Measurement points for the wave elevation (• 1st exp. ∘ 2nd exp.)

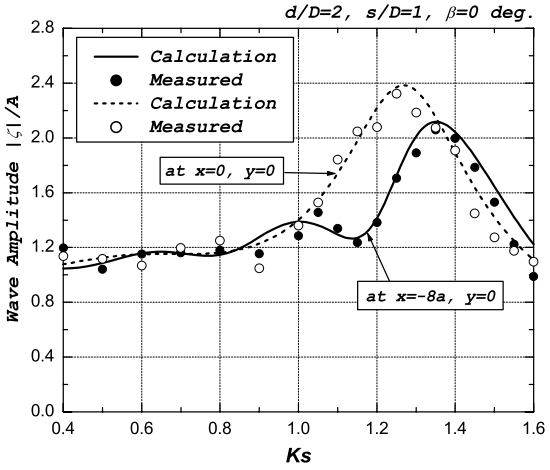

Fig. 3 Wave amplitude on the centerline

wave was measured at an intermediate position between the tested model and the wave generator to minimize the effect of reflected waves from the model.

Due to many measuring points, we had to limit the number of frequencies of the incident wave. For that purpose, preliminary measurements were conducted at 15 positions from the upwave side (using 3 units of the wave measuring apparatus) on the centerline of the array, by changing frequencies with nondimensional wavenumber Ks $(= \omega^2 s/g)$ as a parameter. An example of preliminary measurements is shown in Fig. 3 for the first-order wave amplitude; these are the results at two representative positions of $(x, y) = (-8a, 0)$ and $(0, 0)$. Computed results based on the linear potential theory are also shown in Fig. 3.

We can see good agreement between measured and computed results, which implies reliability of the numerical computation for the first-order boundary-value problem. From these preliminary measurements, three wavenumbers $Ks = 0.8$, 1.2, 1.5 (which correspond to the wavelength of $\lambda/2s = 3.93$, 2.62, 2.09 respectively) were selected for measuring the spatial distribution of the wave elevation.

Measured data were Fourier-analyzed, by taking account of up to the third harmonic of the wave frequency $3\,\omega$. The duration of time in the Fourier analysis was determined on the monitor screen by confirming no obvious effects of reflected waves from side walls of the wave tank. Since there are a great amount of data, only the first- and second-order wave amplitudes will be shown in this paper in nondimensional forms given by

$$\left|\zeta^{(1)}\right|/A, \quad \left|\zeta^{(2)}\right|/KA^2. \tag{1}$$

3. THEORETICAL CALCULATION

With the usual potential-flow assumption, we introduce the velocity potential $\Phi(x, y, z, t)$, satisfying Laplace's equation in the fluid. As shown in Fig. 1, Cartesian coordinates $\boldsymbol{x} = (x, y, z)$ are used, with z pointing vertically upwards.

The solution is assumed to be time-harmonic, so that the time dependence can be factored out. In the monochromatic wave case, if we assume the following perturbation series for the velocity potential

$$\Phi = \epsilon\,\Phi^{(1)}(\boldsymbol{x}, t) + \epsilon^2 \Phi^{(2)}(\boldsymbol{x}, t) + \cdots, \tag{2}$$

the first- and second-order potentials, $\Phi^{(1)}$ and $\Phi^{(2)}$, will have the following form:

$$\Phi^{(1)}(\boldsymbol{x}, t) = \mathrm{Re}\big[\,\phi^{(1)}(\boldsymbol{x})\, e^{i\omega t}\,\big], \tag{3}$$

$$\Phi^{(2)}(\boldsymbol{x}, t) = \overline{\phi}^{(2)}(\boldsymbol{x}) + \mathrm{Re}\big[\,\phi^{(2)}(\boldsymbol{x})\, e^{i2\omega t}\,\big]. \tag{4}$$

The second-order steady component, $\overline{\phi}^{(2)}$ in (4), will not be treated in this paper, because we are interested only in the periodic components.

Corresponding to the experiment condition, only the diffraction problem is considered, so that the periodic components are expressed as

$$\phi^{(j)}(\boldsymbol{x}) = \phi_I^{(j)}(\boldsymbol{x}) + \phi_S^{(j)}(\boldsymbol{x}), \quad j = 1, 2, \tag{5}$$

where $\phi_I^{(j)}(\boldsymbol{x})$ is the incident-wave velocity potential (which will be explicitly given) and $\phi_S^{(j)}(\boldsymbol{x})$ is the scattering potential to be obtained.

Substituting the perturbation series of (2) into the original nonlinear boundary-value problem, we can obtain corresponding boundary-value problems for the velocity potentials at different orders. The details of the derivation are well known and thus we give only the final expressions for the free-surface conditions at first and second order, which are

$$\frac{\partial \phi^{(1)}}{\partial z} - K\,\phi^{(1)} = 0, \tag{6}$$

$$\frac{\partial \phi^{(2)}}{\partial z} - 4K\,\phi^{(2)} = Q(x, y), \tag{7}$$

where

$$Q = -\frac{i\omega}{g}\left[\,\nabla\phi^{(1)} \cdot \nabla\phi^{(1)} - \frac{1}{2}\,\phi^{(1)}\Big(\frac{\partial^2 \phi^{(1)}}{\partial z^2} - K\frac{\partial \phi^{(1)}}{\partial z}\Big)\,\right], \tag{8}$$

$K = \omega^2/g$ is the infinite-depth wavenumber, g is the gravitational acceleration, and these expressions are to be evaluated for $z = 0$. In addition, the velocity potential must satisfy the condition of zero normal velocity on the body surface.

Once the velocity potentials at each order are obtained, it is straightforward to compute the free-surface elevation from Bernoulli's equation. The components at first and second order are given as follows:

$$\zeta^{(1)} = -\frac{i\omega}{g}\,\phi^{(1)}\,, \tag{9}$$

$$\zeta^{(2)} = -\frac{i2\omega}{g}\,\phi^{(2)} - \frac{1}{4g}\nabla\phi^{(1)}\cdot\nabla\phi^{(1)} - \frac{K^2}{2g}\,\phi^{(1)}\phi^{(1)}. \tag{10}$$

These are to be evaluated for $z = 0$.

As the first step of the numerical calculation, the first-order boundary-value problem must be solved, for which Kagemoto & Yue's [2] wave interaction theory is adopted in combination with a quadratic isoparametric boundary-element method for an elementary body of general geometry [3].

A solution method for the second-order boundary-value problem is more complicated, as described by Malenica *et al.* [4] for a simpler case of four bottom-mounted circular cylinders equally spaced around a circle. The basic idea of the solution method considered in the present study is similar to that in Malenica *et al.*, but the solution does not succeed at the present moment.

The wave elevation at second order, given by (10), consists of two different contributions. Thus for convenience in discussion, $\zeta^{(2)}$ is expressed in the form

$$\zeta^{(2)} = \zeta^{(22)} + \zeta^{(21)}, \tag{11}$$

where

$$\zeta^{(22)} = -\frac{i2\omega}{g}\,\phi^{(2)}, \tag{12}$$

$$\zeta^{(21)} = -\frac{1}{4g}\nabla\phi^{(1)}\cdot\nabla\phi^{(1)} - \frac{K^2}{2g}\phi^{(1)}\phi^{(1)} \tag{13}$$

are associated respectively with the second-order potential and with quadratic products of the first-order quantities. The latter is easy to compute, because the first-order solution is semi-analytically given in the wave interaction theory.

4. RESULTS AND DISCUSSION

Because of paucity of space, measured and computed results on the spatial distribution of free-surface elevation will be shown only for the case of $Ks = 1.2$ which is close to a near-trapping frequency. Other results will be presented at the Workshop.

Figure 4 shows the nondimensional amplitude of the first-order wave elevation, with the upper figure for computed results based on a linear potential theory, and the middle and lower figures for measured results at wave steepness of $H/\lambda \simeq 1/50$ and $1/20$, respectively. To make it clear the spatial distribution, computed results are shown for $-10 \le x/a \le 10$ and $0 \le y/a \le 3$ which is wider than the area in the measurements. The second-order results are shown in Fig 5 in the same manner. However computed results are only for $|\zeta^{(21)}|/KA^2$ in (11), that is, quadratic products of the first-order quantities.

We can see that the first-order wave becomes large in an interior region between cylinders, indicating that $Ks = 1.2$ is close to a near-trapping frequency of Neumann type discussed by Maniar & Newman [5]. At this wavenumber, computed results of $|\zeta^{(1)}|/A$ seem to be in good agreement with the results measured at $H/\lambda \simeq 1/20$ rather than with the results measured at $H/\lambda \simeq 1/50$ in the linear regime, especially for amplified waves between cylinders. However, this is obviously not the case in the upwave region of the upwavemost cylinder.

Regarding the results of second order, we can see at first glance that the computed results for quadratic products of the first-order quantities, $|\zeta^{(21)}|/KA^2$, are remarkably different from the total second-order wave amplitude $|\zeta^{(2)}|/KA^2$ obtained by the measurement. This fact implies that the second-order component $\zeta^{(22)}$ is similarly large, but its phase relative to $\zeta^{(21)}$ is such that the total second-order wave elevation is not especially large around the first-order near trapping frequency. In a region just beside each cylinder, $|\zeta^{(21)}|$ is small whereas the total wave amplitude $|\zeta^{(2)}|$ is large, which means that the second-order component $\zeta^{(22)}$ is dominant in this region. We can also observe a tendency from measured results that the total second-order wave amplitude becomes large in a region where the first-order wave amplitude takes local maximum or minimum, except for the runup on the upwave face of the upwavemost cylinder.

Concerning the difference in the results measured at $H/\lambda \simeq 1/50$ and $1/20$, the nondimensional value of $|\zeta^{(2)}|/KA^2$ is almost the same, which confirms validity of the perturbation series of physical quantities in terms of the maximum wave slope KA.

5. CONCLUSIONS

To have a clear understanding on the wave interactions among multiple columns of an ocean structure, spatially dense measurements have been carried out for the wave elevation around an array of equally spaced four truncated circular cylinders at various wave frequencies including near-trapped modes. Numerical computations corresponding to the experiments have also been performed. With these results, discussion has been made on the degree of agreement in the first-order wave elevation and on nonlinear effects and their characteristics.

The results obtained in the present study can be summarized as follows:

1) The overall agreement for the first-order wave elevation is very good between computed and measured results. Around the first-order near-trapping frequency, computed results of $|\zeta^{(1)}|/A$ seem to be supported by the measured results in a steeper incident wave of $H/\lambda \simeq 1/20$ rather than the results in a wave of $H/\lambda \simeq 1/50$ appropriate for linear theories.

2) The amplitude of the second-order wave component from quadratic products of the first-order quantities, $|\zeta^{(21)}|$, has a similar spatial distribution to that in the first-order wave amplitude; which is however markedly different from the total second-order wave amplitude $|\zeta^{(2)}|$ obtained by the measurement. This implies that another second-order component to be computed from the second-order potential is also large, thereby canceling or dominating $\zeta^{(21)}$. This cancellation seems to be remarkable at $Ks = 1.2$ close to the first-order near-trapping frequency.

3) Measured results show that the total second-order wave amplitude $|\zeta^{(2)}|$ becomes large in a region where the first-order wave amplitude $|\zeta^{(1)}|$ takes local maximum or minimum, except for the runup on the upwave face of the upwavemost cylinder.

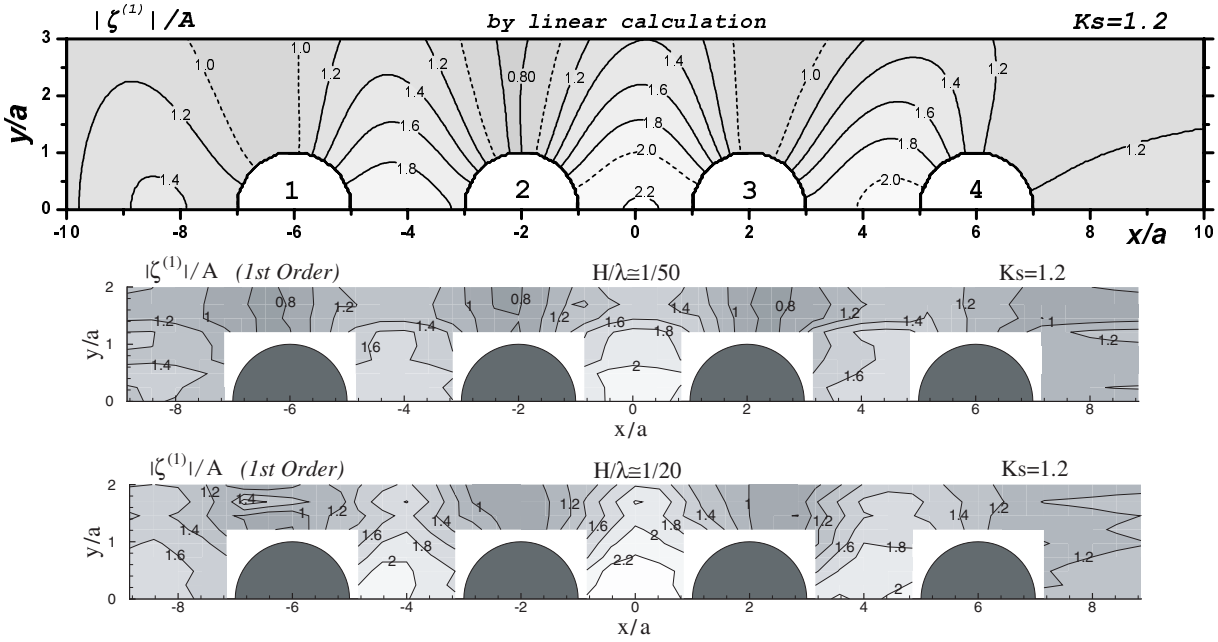

Fig. 4 Amplitude of the first-order wave elevation at $Ks = 1.2$ (upper: computed by linear theory, middle: measured at $H/\lambda \simeq 1/50$, lower: measured at $H/\lambda \simeq 1/20$)

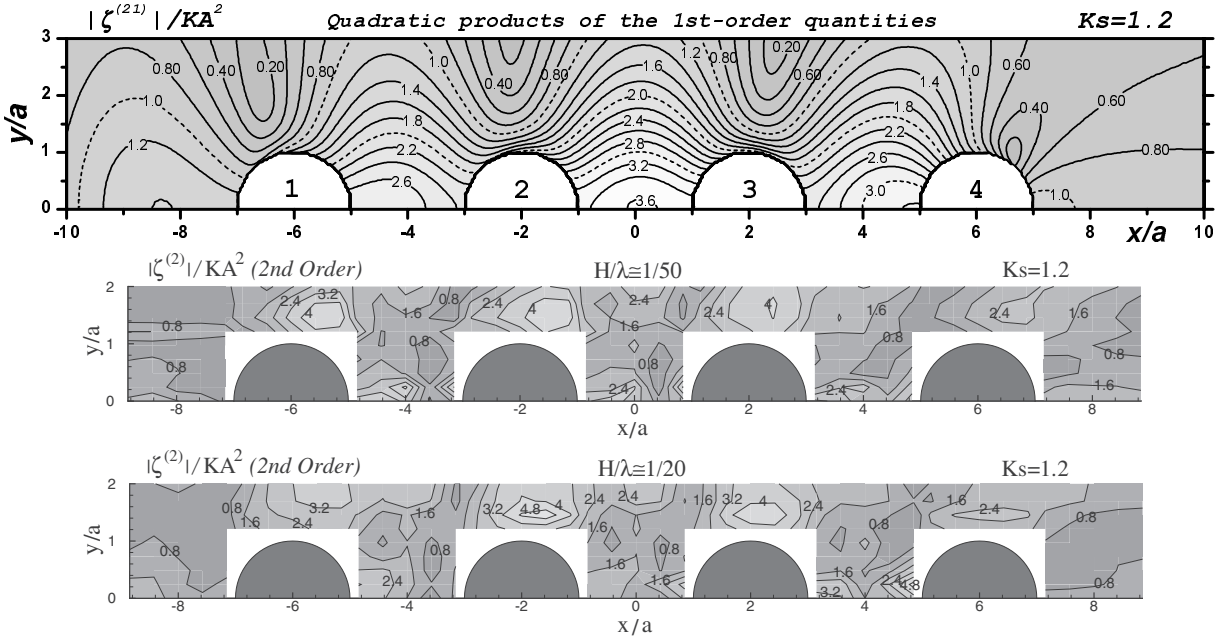

Fig. 5 Amplitude of the second-order wave elevation at $Ks = 1.2$ (upper: computed results for quadratic products of the first-order quantities, middle: measured at $H/\lambda \simeq 1/50$, lower: measured at $H/\lambda \simeq 1/20$)

REFERENCES

[1] Kashiwagi, M and Yoshida, S (1998). "Hydrodynamic Interactions among Multiple Floating Cylinders in a Regular Arrangement", *Proc of 15th Ocean Eng Symp*, Soc of Naval Arch of Japan, pp 231–238

[2] Kagemoto, H and Yue, DKP (1986). "Interactions among Multiple Three-Dimensional Bodies in Water Waves: An Exact Algebraic Method", *Journal of Fluid Mechanics*, Vol 166, pp 189–209

[3] Kashiwagi, M and Kohjoh, T (1995). "A Method of Computing Hydrodynamic Interactions in Large Floating Structures Composed of Multiple Bodies", *Proc of 13th Ocean Eng Symp*, Soc of Naval Arch of Japan, pp 247–254

[4] Malenica, S, Eatock Taylor, R and Hung, JB (1999). "Second-Order Water Wave Diffraction by an Array of Vertical Cylinders", *Journal of Fluid Mechanics*, Vol 390, pp 349–373

[5] Maniar, HD and Newman, JN (1997). "Wave Diffraction by a Long Array of Cylinders", *Journal of Fluid Mechanics*, Vol 339, pp 309–330

17thIWWWFB

Discussion Sheet

Abstract Title :	First- and second-order water waves around an array of floating vertical cylinders		
(Or) Proceedings Paper No. :	19	***Page :***	073
First Author :	Kashiwagi, M.		
Discusser :	David V. Evans		

Questions / Comments :

The occurance of large amplitudes on cylinders near the centre of a symmetric linear array arrises from the existence of a pure linear trapped mode for a simple cylinder in a narrow channel. It would be of interest to consider the possibility of second-order trapped modes for this configuration.

Author's Reply :
(If Available)

As shown in the measured results, the second-order wave amplitudes at the frequency where the first-order wave amplitudes become large are small due to cancellation between the components to be computed from the second-order velocity potential and the quadratic products of the first-order quantities. According to the work by Malenica and Eatock Taylor, the second-order trapped mode will occur at half of the first-order trapped-mode frequency, which should be confirmed by experiments and also by numerical calculations for the present configuration.